Comput Mech (2005) 37: 70–77
DOI 10.1007/s00466-005-0699-9

ORIGINAL PAPER

M. Schanz · T. Rüberg · V. Struckmeier

# Quasi-static poroelastic boundary element formulation based on the convolution quadrature method

Received: 25 May 2004 / Revised: 15 February 2005 / Published online: 4 June 2005


**Abstract** Convolution Quadrature Method (CQM)-based Boundary Element formulations are up to now used only in dynamic formulations. The main difference to usual time-stepping BE formulations is the way to solve the convolution integral appearing in most time-dependent integral equations. In the CQM formulation, this convolution integral is approximated by a quadrature rule whose weights are determined by the Laplace transformed fundamental solutions and a linear multi-step method.

In principle, for quasi-static poroelasticity there is no need to apply the CQM because time-dependent fundamental solutions are available. However, these fundamental solutions are highly complicated yielding very sensitive algorithms. On the contrary, the CQM based BE formulation proposed here is very robust and yields comparable results to other methodologies. This formulation is tested in 2-d in comparison with a Finite Element Method and analytical results.

## 1 Introduction

Convolution Quadrature Method (CQM)-based Boundary Element (BE) formulations are first published in 1997 [19, 20] with applications in elasto- or viscoelastodynamics. The main difference to usual time-stepping BE formulations is the way to solve the convolution integral appearing in most time-dependent integral equations. In the CQM formulation, this convolution integral is approximated by a quadrature rule whose weights are determined by the Laplace transformed fundamental solutions and a multi-step method [13, 14]. An overview of this BE formulation is given in [18].

There are mainly two reasons to use a CQM-based BEM instead of usual time-stepping procedures. One reason is to improve the stability of the time-stepping procedure [19, 1]. The other reason is to tackle problems where no time-dependent fundamental solutions are available, e.g., for inelastic material behavior in viscoelastodynamics [16], in poroelastodynamics [17], or for functional graded materials [25]. Also, this method is used to avoid highly complicated fundamental solutions in time domain [2, 23, 24].

However, up to now, the CQM-based BEM is used only in dynamic formulations. Clearly, for quasi-static problems in poroelasticity there is no need to apply the CQM because time-dependent fundamental solutions are available [7]. However, these fundamental solutions are highly complicated yielding very sensitive algorithms. Therefore, it is promising to apply the CQM also to the quasi-static integral equations in poroelasticity. This approach is presented for quasi-static viscoelasticity and poroelasticity for 3-dimensional continua in [21]. Here, the 2-d case for poroelasticity is discussed.

Here, at first, poroelastic constitutive equations are recalled based on Biot's theory [3]. It should be mentioned that the proposed method can also be applied to mixture theory based theories as the Theory of Porous Media [8] because the mathematical operator of the governing equations is equal to that of Biot's theory, as shown for the dynamic case by Schanz and Diebels [22]. The singular behavior of the 2-d fundamental solutions in Laplace domain is discussed. The explicit expressions of these quasi-static fundamental solutions in Laplace domain may be found in [5] or the respective time domain solutions in the survey article by Cheng and Detournay [6].

Subsequent to the formulation of the constitutive and governing equations, the respective integral equations

M. Schanz (✉)
Institute of Applied Mechanics,
Graz University of Technology,
Technikerstr. 4, 8010 Graz, Austria
E-mail: m.schanz@tugraz.at
Tel.: +43-316-8737600
Fax: +43-316-8737641

T. Rüberg · V. Struckmeier
Institute of Applied Mechanics,
Technical University Braunschweig,
P.O. Box 3329, D-38023 Braunschweig, Germany

are presented. Applying the usual spatial discretization and using the CQM for the temporal discretization yields the final time-stepping algorithm. The proposed methodology is tested for consolidation processes in comparison with analytical solutions and a FE formulation for the example of a soil column and the borehole problem.

Throughout this paper, the summation convention is applied over repeated indices and Latin indices receive the values 1 and 2 in two-dimensions (2-d). Commas $()_{,i}$ denote spatial derivatives and, as usual, the Kronecker delta is denoted by $\delta_{ij}$.

## 2 Governing equations and fundamental solutions

In the following, the constitutive equations and the governing equations for a poroelastic continuum are given in a short form. The intention is only to point out the notation and to state the basic assumptions. For a more detailed description on poroelasticity the reader is referred to Biot's original work [3] or to the quite comprehensive article of Detournay and Cheng [10]. Further, as the CQM uses fundamental solutions only in Laplace domain, it is sufficient to give the governing equations and their fundamental solutions in Laplace domain.

Following Biot's approach to model the behavior of porous media, the constitutive equations can be expressed as

$$\sigma_{ij} = G\left(u_{i,j} + u_{j,i}\right) + \frac{2Gv}{1-2v}\delta_{ij}u_{k,k} - \alpha\delta_{ij}p$$
$$\zeta = \alpha u_{k,k} + \frac{\alpha^2(1-2v_u)(1-2v)}{2G(v_u - v)}p \tag{1}$$

in which $\sigma_{ij}$ denotes the total stress, $p$ the pore pressure, $u_i$ the displacements of the solid frame, and $\zeta$ the variation of fluid volume per unit reference volume. The sign convention for stress and strain follows that of elasticity, namely, tensile stress and strain is denoted positive. The bulk material is defined by the shear modulus $G$ and Poisson ratio $v$, known from elasticity. The porosity $\phi$, Biot's effective stress coefficient $\alpha$, and the undrained Poisson's ratio $v_u$ complete the set of material parameters. Further, a linear strain-displacement relation $\varepsilon_{ij} = 1/2\left(u_{i,j} + u_{j,i}\right)$ is used, i.e., small deformation gradients are assumed.

Conservation of the linear momentum yields the static equilibrium

$$\sigma_{ij,j} = -F_i \tag{2}$$

formulated for the mixture, i.e., for the solid and the interstitial fluid. In Eq. (2), $F_i$ denotes the bulk body forces. The mass conservation is governed by the continuity equation

$$\frac{\partial}{\partial t}\zeta + q_{i,i} = a, \tag{3}$$

with the specific flux of the fluid $q_i$ and a source term $a(t)$. Finally, the interstitial flow is modeled with Darcy's law

$$q_i = -\kappa p_{,i} \tag{4}$$

where $\kappa$ denotes the permeability.

As shown in [4], it is sufficient to use the solid displacement and the pore pressure as basic variables to describe a poroelastic continuum. Therefore, the above equations are reduced to these three unknowns. Clearly, contrary to the dynamic case, this can be achieved even in time domain by eliminating the flux in the above given equations. However, because in the following only the Laplace transformed equations are necessary, equations (1) — (4) are transformed to Laplace domain. Subsequently, eliminating the flux yields the final set of differential equations for the displacements $\hat{u}_i$ and the pore pressure $\hat{p}$

$$G\hat{u}_{i,jj} + \frac{G}{1-2v}\hat{u}_{j,ij} - \alpha\hat{p}_{,i} = -\hat{F}_i \tag{5a}$$

$$\kappa\hat{p}_{,ii} - \frac{s\alpha^2(1-2v_u)(1-2v)}{2G(v_u-v)}\hat{p} - \alpha s\hat{u}_{i,i} = -\hat{a}, \tag{5b}$$

where $\hat{f}(s)$ denotes the Laplace transform of a function $f(t)$ with the complex Laplace variable $s$. It must be mentioned that vanishing initial conditions for all state variables are assumed.

The fundamental solutions for the system of governing equations (5) are solutions due to single forces in the solid in all two spatial directions $\hat{F}_i\mathbf{e}_j = \delta(\mathbf{x}-\mathbf{y})\delta_{ij}$ denoted by $\hat{U}^S_{ij}$ and $\hat{P}^S_i$ as well due to a single source in the fluid $\hat{a} = \delta(\mathbf{x}-\mathbf{y})$ denoted by $\hat{U}^F_i$ and $\hat{P}^F$, i.e., in total four functions. These solutions can be found in the literature, e.g., in [5], and are presented for convenience in the Appendix A. For developing a BE formulation the corresponding integral equation to the system (5) is used. There, an essential feature is the singular behavior of the fundamental solutions and their derivatives, i.e., the flux and the traction fundamental solution. Simple series expansion with respect to the variable $r = |\mathbf{x}-\mathbf{y}|$ shows that these solutions behave in the limit $r \to 0$ like the elastic or the acoustic fundamental solutions, i.e.,

$$\hat{U}^S_{ij} = \frac{1}{8\pi G(1-v)}\left\{r_{,i}r_{,j} - \delta_{ij}\ln r(3-4v)\right\} + \mathcal{O}\left(r^0\right) \tag{6a}$$

$$\hat{P}^F = \frac{-1}{2\pi\kappa}\ln r + \mathcal{O}\left(r^0\right) \tag{6b}$$

$$\hat{T}^S_{ij} = \frac{-1}{4\pi(1-v)r}\left\{\left[(1-2v)\delta_{ij} + 2r_{,i}r_{,j}\right]r_{,n} - (1-2v)\left(r_{,j}n_i - r_{,i}n_j\right)\right\} + \mathcal{O}\left(r^0\right) \tag{6c}$$

$$\hat{T}^F_i = \frac{-s\alpha(1-2v)}{4\pi\kappa(1-v)}n_i\ln r + \mathcal{O}\left(r^0\right) \tag{6d}$$

$$\hat{Q}^S_j = \frac{\alpha(1-2v)}{8\pi G(1-v)}n_j\ln r + \mathcal{O}\left(r^0\right) \tag{6e}$$

$$\hat{Q}^F = -\frac{1}{2\pi}\frac{r_{,n}}{r} + \mathcal{O}\left(r^0\right). \tag{6f}$$

In Eqs. (6), $r_{,n} = r_{,k}n_k$ denotes the normal derivative and the fundamental solutions $\hat{U}_i^F = s\hat{P}_i^S = \mathcal{O}(r^0)$ are regular. Further, $\hat{T}_{ij}^S, \hat{Q}_j^S$ and $\hat{T}_i^F, \hat{Q}^F$ in (6) are traction or flux fundamental solutions due to a single force in the solid (superscript $S$) or a source in the fluid (superscript $F$), respectively.

## 3 Quasi-static Boundary Element formulation

To establish a BE formulation an integral equation corresponding to the governing equations must be derived. Starting from a weighted residual statement defined on the domain $\Omega$ with boundary $\Gamma$ using fundamental solutions as weighting functions an integral equation is achieved. Next, performing two partial integrations with respect to the spatial variable yields the boundary integral equations. With careful regard to the singular behavior of the fundamental solutions, the load point $\mathbf{y}$ is shifted to the boundary. Based on the system of Eqs. (5), the integral equations for poroelasticity

$$\int_\Gamma \begin{bmatrix} U_{ij}^S(t,\mathbf{y},\mathbf{x}) & -P_j^S(t,\mathbf{y},\mathbf{x}) \\ U_i^F(t,\mathbf{y},\mathbf{x}) & -P^F(t,\mathbf{y},\mathbf{x}) \end{bmatrix} * \begin{bmatrix} t_i(t,\mathbf{x}) \\ q(t,\mathbf{x}) \end{bmatrix} \mathrm{d}\Gamma - \oint_\Gamma \begin{bmatrix} T_{ij}^S(t,\mathbf{y},\mathbf{x}) & Q_j^S(t,\mathbf{y},\mathbf{x}) \\ T_i^F(t,\mathbf{y},\mathbf{x}) & Q^F(t,\mathbf{y},\mathbf{x}) \end{bmatrix} * \begin{bmatrix} u_i(t,\mathbf{x}) \\ p(t,\mathbf{x}) \end{bmatrix} \mathrm{d}\Gamma = \begin{bmatrix} c_{ij}(\mathbf{y}) & 0 \\ 0 & c(\mathbf{y}) \end{bmatrix} \begin{bmatrix} u_i(t,\mathbf{y}) \\ p(t,\mathbf{y}) \end{bmatrix}. \tag{7}$$

are achieved. The integral free terms $c_{ij}$ and $c$ are due to the strongly singular behavior of the second integral in (7) where $\oint$ denotes the Cauchy principal value of the integral. As seen from the singular parts of the traction fundamental solutions (6c) and the flux fundamental solution (6f), the integral free terms $c_{ij}$ are equal to elastostatics and acoustics, i.e., $c_{ij} = 1/2\delta_{ij}$ and $c = 1/2$ for a smooth boundary. For corners or edges the procedure proposed by Mantic [15] to determine these terms can be used. Further, the expressions $T_{ij}^S, T_i^F, Q_j^S$, and $Q^F$ are introduced during the derivation of the integral Eq. (7) (see appendix A). The time domain representation is obtained by a formal inverse Laplace transform where all products between two Laplace parameter dependent functions are transformed into convolution integrals

$$f * g = \int_0^t f(t-\tau)g(\tau)\mathrm{d}\tau. \tag{8}$$

Next, a boundary element formulation is achieved following the usual procedure, i.e., introducing spatial and temporal discretization.

### 3.1 Spatial discretization

First, the boundary surface $\Gamma$ is discretized by $E$ isoparametric elements $\Gamma_e$ where $F$ polynomial shape functions $N_e^f(\mathbf{x})$ are defined. Hence, the following ansatz functions with the time-dependent nodal values $u_i^{ef}(t)$, $t_i^{ef}(t)$, $p^{ef}(t)$, and $q^{ef}(t)$ are used to approximate the boundary states

$$\begin{aligned} u_i(\mathbf{x},t) &= \sum_{e=1}^{E}\sum_{f=1}^{F} N_e^f(\mathbf{x})u_i^{ef}(t), \\ t_i(\mathbf{x},t) &= \sum_{e=1}^{E}\sum_{f=1}^{F} N_e^f(\mathbf{x})t_i^{ef}(t), \\ p(\mathbf{x},t) &= \sum_{e=1}^{E}\sum_{f=1}^{F} N_e^f(\mathbf{x})p^{ef}(t), \\ q(\mathbf{x},t) &= \sum_{e=1}^{E}\sum_{f=1}^{F} N_e^f(\mathbf{x})q^{ef}(t). \end{aligned} \tag{9}$$

In Eq. (9), the shape functions of all four variables are denoted by the same function $N_e^f(\mathbf{x})$ indicating the same approximation level for all variables. This is not mandatory but usual. Inserting these ansatz functions (9) in the time dependent integral Eq. (7) yields

$$\sum_{e=1}^{E}\sum_{f=1}^{F}\left\{ \int_\Gamma \begin{bmatrix} U_{ij}^S(r,t) & -P_j^S(r,t) \\ U_i^F(r,t) & -P^F(r,t) \end{bmatrix} N_e^f(\mathbf{x})\mathrm{d}\Gamma * \begin{bmatrix} t_i^{ef}(t) \\ q^{ef}(t) \end{bmatrix} - \int_\Gamma \begin{bmatrix} T_{ij}^S(r,t) & Q_j^S(r,t) \\ T_i^F(r,t) & Q^F(r,t) \end{bmatrix} N_e^f(\mathbf{x})\mathrm{d}\Gamma * \begin{bmatrix} u_i^{ef}(t) \\ p^{ef}(t) \end{bmatrix} \right\} = \begin{bmatrix} c_{ij}(\mathbf{y}) & 0 \\ 0 & c(\mathbf{y}) \end{bmatrix} \begin{bmatrix} u_i(\mathbf{y},t) \\ p(\mathbf{y},t) \end{bmatrix}. \tag{10}$$

### 3.2 Temporal discretization

Next, a time discretization has to be introduced. Instead of using the time-dependent fundamental solutions, here, the convolution quadrature method (briefly summarized in Appendix B) is used as a promising alternative.

Hence, after dividing time period $t$ in $N$ time steps of equal duration $\Delta t$, so that $t = N\Delta t$, the convolution integrals between the fundamental solutions and the nodal values in (10) are approximated by the convolution quadrature method, i.e., the quadrature formula (21) is applied to the integral equation Eq. (10). This results in the following boundary element time stepping procedure ($n = 0, 1, \ldots, N$)

$$\sum_{e=1}^{E}\sum_{f=1}^{F}\sum_{k=0}^{n}\left\{ \begin{bmatrix} \omega_{n-k}^{ef}\left(\hat{U}_{ij}^S\right) & -\omega_{n-k}^{ef}\left(\hat{P}_j^S\right) \\ \omega_{n-k}^{ef}\left(\hat{U}_i^F\right) & -\omega_{n-k}^{ef}\left(\hat{P}^F\right) \end{bmatrix} \begin{bmatrix} t_i^{ef}(k\Delta t) \\ q^{ef}(k\Delta t) \end{bmatrix} - \begin{bmatrix} \omega_{n-k}^{ef}\left(\hat{T}_{ij}^S\right) & \omega_{n-k}^{ef}\left(\hat{Q}_j^S\right) \\ \omega_{n-k}^{ef}\left(\hat{T}_i^F\right) & \omega_{n-k}^{ef}\left(\hat{Q}^F\right) \end{bmatrix} \begin{bmatrix} u_i^{ef}(k\Delta t) \\ p^{ef}(k\Delta t) \end{bmatrix} \right\} = \begin{bmatrix} c_{ij}(\mathbf{y}) & 0 \\ 0 & c(\mathbf{y}) \end{bmatrix} \begin{bmatrix} u_i(n\Delta t) \\ p(n\Delta t) \end{bmatrix} \tag{11}$$

**Table 1** Material data of a soil (coarse sand)

| G $\left(\frac{N}{m^2}\right)$ | $\nu$ | $\phi$ | $\alpha$ | $\nu_u$ | $\kappa\left(\frac{m^4}{N\,s}\right)$ |
|---|---|---|---|---|---|
| $9.8 \cdot 10^7$ | 0.298 | 0.48 | 0.980918 | 0.49 | $3.55 \cdot 10^{-9}$ |

with the integration weights corresponding to (23), e.g.,

$$\omega_n^{ef}\left(\hat{U}_{ij}^S, \mathbf{y}, \Delta t\right) = \frac{\mathscr{R}^{-n}}{L}\sum_{\ell=0}^{L-1}\int_\Gamma \hat{U}_{ij}^S\left(\mathbf{x}, \mathbf{y}, \frac{\gamma\left(\mathscr{R}e^{i\ell\frac{2\pi}{L}}\right)}{\Delta t}\right) \times N_e^f(\mathbf{x})\,\mathrm{d}\Gamma\,\mathrm{e}^{-in\ell\frac{2\pi}{L}}. \tag{12}$$

Note, the calculation of the integration weights is only based on the Laplace transformed fundamental solutions. Therefore, with this time stepping procedure (11), a boundary element formulation for quasi-static poroelasticity is given without time-dependent fundamental solutions.

To calculate the integration weights $\omega_{n-k}^{ef}$ in (11), spatial integration over the boundary $\Gamma$ has to be performed. The regular integrals are evaluated by standard Gaussian quadrature rule. The weakly and strongly singular parts of the integrals in (11) are solved analytically for linear elements. Moreover, to obtain a system of algebraic equations, collocation is used at every node of the shape functions $N_e^f(\mathbf{x})$.

According to $t - \tau = (n-k)\Delta t$, the integration weights $\omega_{n-k}^{ef}$ are only dependent on the difference $n-k$. This property is analogous to elastodynamic time domain BE formulations (see, e.g., [11]) and can be used to establish a recursion formula for $n = 1, 2, \ldots, N$ $(m = n - k)$

$$\omega_0(\mathbf{C})\mathbf{d}^n = \omega_0(\mathbf{D})\bar{\mathbf{d}}^n + \sum_{m=1}^{n}(\omega_m(\mathbf{U})\mathbf{t}^{n-m} - \omega_m(\mathbf{T})\mathbf{u}^{n-m}). \tag{13}$$

with the time dependent integration weights $\omega_m$ containing the Laplace transformed fundamental solutions. Similarly, $\omega_0(\mathbf{C})$ and $\omega_0(\mathbf{D})$ are the corresponding integration weights of the first time step related to the unknown boundary data $\mathbf{d}^n$ and the known boundary data $\bar{\mathbf{d}}^n$ in the time step $n$, respectively. Finally, a direct equation solver is applied.

## 4 Example: Poroelastic column and borehole

To show the accuracy and the robustness of the proposed formulation, the displacement response and the pore pressure distribution of a 2-d bar is compared with an analytical solution [10] and a Finite Element (FEM)[1] calculation. Further, the displacement and pressure results from a borehole are compared with the analytical result [9]. The used material data in both test examples are those of a soil (see Table 1) which can be found in the literature [12].

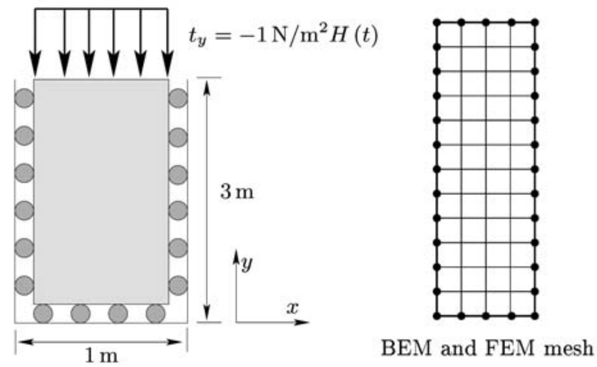


**Fig. 1** Geometry, loading, and discretization of the 2-d bar

*Poroelastic column* First, a bounded domain is chosen as test example to have the possibility not only to compare with an analytical solution but also with the other competitive method, the FEM. For this purpose, a 2-d bar (3 m × 1 m) is considered (see Fig. 1). This bar is fixed at one end and loaded with $t_y = -1$ N/m$^2$ $H(t)$ over the whole time period on the other end. At the other surfaces the normal displacements are blocked and in tangential directions free sliding, i.e., zero traction, is modeled. Further, the free surface where the load as total stress function is applied is assumed to be permeable, i.e., the prescribed pore pressure vanishes. All other surfaces including the fixed end are impermeable, i.e., the flux vanishes there. The geometry and the meshes of the FEM and BEM calculation are shown in Fig. 1. There, the bullets on the boundary indicate the 32 linear elements used for the BEM, and the thin lines the 48 linear elements for the FEM.

In Fig. 2, the calculated vertical displacements at the middle point of the free and loaded surface are plotted versus time for the analytical solution, the proposed BE formulation, and the FE formulation. The poroelastic analytical 1-d solution is taken from the literature [10].

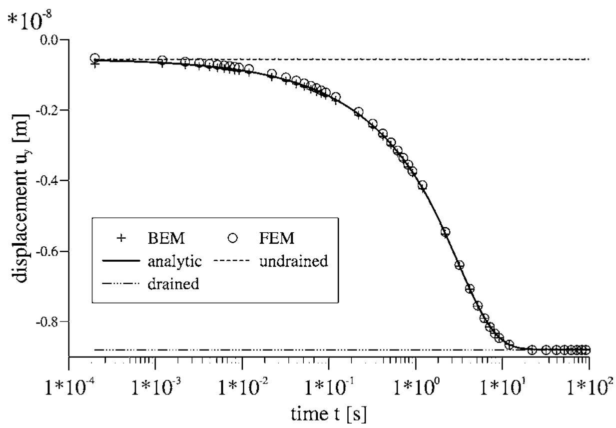


**Fig. 2** Displacement at the free end of the bar versus time: BEM results compared with FEM results and the analytical solution (log-scale in time)

[1]The FEM code DIANA-SWANDYNE II from http://www.bham.ac.uk/CivEng/swandyne is used

The time axis is divided in a logarithmic scale to present a large range of observation time.

Additionally to the poroelastic results, as upper and lower bounds two elastostatic solutions are presented, i.e., the drained and undrained elastostatic solution are given for comparison. Both numerical solutions agree well with the analytical result and coincide with the undrained solutions for small times and with the drained solution for large times. However, for small times the BEM results come a bit closer to the analytical result than the FEM solution. Overall, both numerical methods are suitable to treat this problem even with the chosen coarse meshes. It should be mentioned that the time step size in the BE formulation has nearly no influence on the results and no stability problems occur if the time step size is chosen large enough to resolve the physical phenomenon.

Next, in Fig. 3 the pressure solution for both methods and the analytical result is plotted along the mid-line of the bar for three different times ($t = 0.1$ s, $t = 1$ s, and $t = 10$ s).

Some deviations between the FEM and BEM results are observed but only for smaller times and there only close to the support. The BEM is even closer to the analytical solution than the FEM solution. Even, the steep descent at the free surface is captured well.

*Borehole problem* Next, an unbounded domain is considered where a borehole is drilled. Clearly, for such a task only the BEM is suitable and no longer the FEM due to the necessity of mesh truncation. Therefore, here, only the comparison with the analytical solution [9] is presented. Further, as discussed in [5], this problem can be analyzed by assuming plain strain conditions, provided that one of the principal stress axes is parallel to the borehole axis, and the time needed to drill the distance of about five times the radius $a$ of the borehole is much smaller than the characteristic time $a^2/c$.

Here, the so-called third mode is tackled, i.e., the loading of the borehole is a far-field deviatoric stress (see Fig. 4). It is assumed that the borehole is drilled instantaneously at $t = 0$ s and that the shear stress and the pore pressure are brought to zero at the borehole wall for $t > 0$ s. This loading scenario is realized by solving a problem for the boundary conditions at the borehole wall

$$\sigma_{rr} = S^0 \cos 2\theta \quad \sigma_{r\theta} = -S^0 \sin 2\theta \quad p = 0N/m^2 \tag{14}$$

with the polar coordinates $r$ and $\theta$. The magnitude of the in-plane far-field deviator stress is chosen $S^0 = 1$ N/m$^2$. Afterwards the background stresses are superposed.

In the BEM solution the borehole perimeter is subdivided in 64 linear elements. The radius of the borehole is set to $a = 1$ m. The material is, as before, a soil (see table 1). Together with the displacement solution at the point $P$ the original and deformed geometry is given in Fig. 4. The deformed geometry (the dashed line) is as expected an ellipse corresponding to the pressure and tensile parts of the load. Further, in Fig. 4 the time history of the displacement at the borehole wall is depicted versus time. The time axis is given in a logarithmic scale to present a large time range. The BEM result agrees very well with the analytical solution independently whether small or large times are considered.

Next, in Fig. 5 the pressure distribution is given along a line heading at point $P$ and going along the radial direction ($\theta = 0°$) up to a distance of $r = 2$ m for four different times $t = 0.01$ s, $t = 0.1$ s, $t = 1$ s, and $t = 10$ s. A perfect agreement with the analytical results is observed.

## 5 Conclusions

An application of the CQM to quasi-static problems in poroelasticity is presented. Following the procedure known from the corresponding dynamic BE formulations, a time stepping BE formulation based on the Laplace transformed fundamental solutions and on a

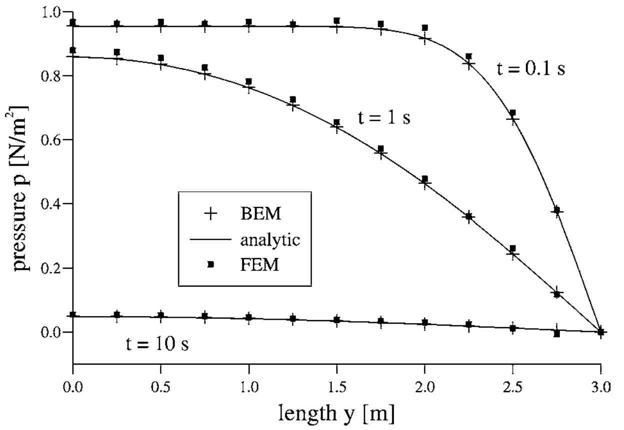


**Fig. 3** Pressure distribution along the mid-line of the bar: BEM results compared with FEM results and the analytical solution for different times

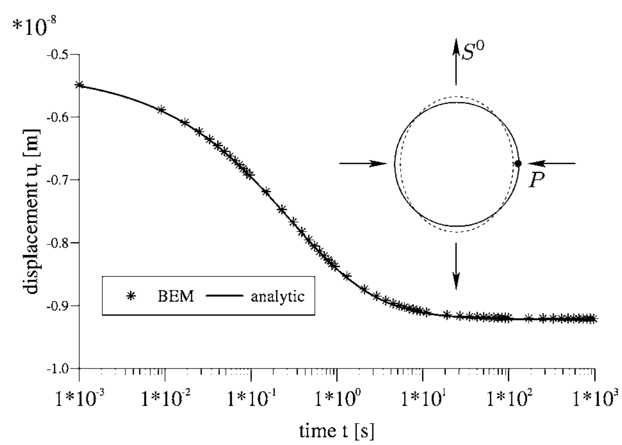


**Fig. 4** Displacement at point $P$ of the borehole versus time: BEM results compared with the analytical solution (log-scale in time)

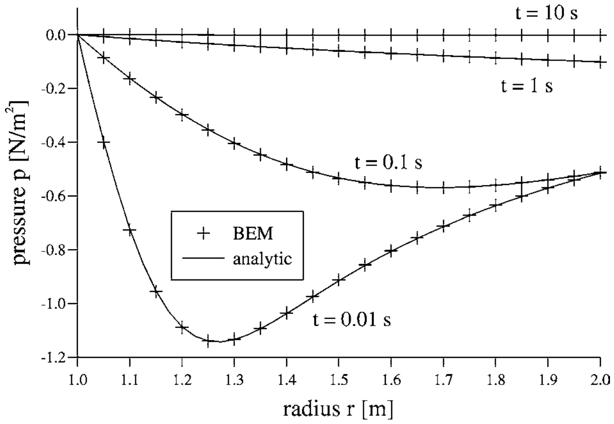


**Fig. 5** Pressure distribution along a line starting from point $P$ radial to the borehole: BEM results compared with the analytical solution

linear multi-step method is established. Hence, only the Laplace domain fundamental solutions are necessary which can be derived much easier than in time domain.

Numerical studies have shown that the proposed poroelastic BE formulation is very robust and accurate. Studies concerning spatial and temporal discretization were presented in a former paper [21] which have shown that the proposed formulation is nearly independent of the chosen time step size if, especially in 3-d, a satisfactory spatial discretization is chosen. Here, the numerical studies are restricted to the 2-d case where the numerical results can be checked with analytical solutions. The comparison of results achieved for a soil column and a borehole under mode 3 loading show a very good agreement. Further, these calculations are compared for the column with a FEM calculation also showing good agreement. It should be remarked that no dependence on the time step size or any instabilities are observed in the proposed formulation.

**Acknowledgements** The financial support by the German Research Foundation (DFG) under grant SCHA 527/5-2 and of the GRK 802 *Riscmanagement* is gratefully acknowledged.

## Appendix

### A Poroelastic fundamental solutions

In the following, the explicit expressions of the poroelastic quasi-static fundamental solutions in 2-d are given. A collection of all types of time-dependent fundamental solutions caused by different loads for a quasi-static poroelastic modeled continuum can be found in [6]. The Laplace transformed solutions presented here are taken from [5].

The displacement and the pressure due to a single source in the solid are

$$\begin{aligned}\hat{U}^S_{ij} = \frac{1}{2\pi}\Bigg\{ &-\frac{3-4\nu_u}{4G(1-\nu_u)}\delta_{ij}\ \mathrm{In}\ r + \frac{1}{4G(1-\nu_u)} r_{,i}\, r_{,j} \\ &+ \frac{\nu_u-\nu}{2G(1-\nu)(1-\nu_u)}\left[\delta_{ij}\left(\xi^{-2}-\xi^{-1}K_1(\xi)\right)\right. \\ &\left.+ r_{,i}\, r_{,j}\left(K_2(\xi)-2\xi^{-2}\right)\right]\Bigg\}\end{aligned} \tag{15}$$

$$\hat{P}^S_i = \frac{1}{2\pi}\frac{\nu_u-\nu}{s\alpha(1-2\nu)(1-\nu_u)}\lambda r_{,i}\left(K_1(\xi)-\xi^{-1}\right) \tag{16}$$

and due to a source in the fluid are

$$\hat{U}^F_i = \frac{1}{2\pi}\frac{\nu_u-\nu}{\alpha(1-2\nu)(1-\nu_u)}\lambda r_{,i}\left(K_1(\xi)-\xi^{-1}\right) \tag{17}$$

$$\hat{P}^F = \frac{1}{2\pi\kappa}K_0(\xi) \tag{18}$$

with $\lambda^2 = \frac{s\alpha^2(1-\nu_u)(1-2\nu)^2}{2\kappa G(1-\nu)(\nu_u-\nu)} = \frac{s}{c}$ and $\xi = r\lambda$. Further, the $K_i$'s denote the modified Bessel functions of second kind.

During derivation of the boundary integral equation from the weighted residual statement two integrations by part have to be performed. For convenience and also with a physical interpretation of an 'adjoint' traction or flux the following abbreviations are introduced

$$\begin{aligned}\hat{T}^S_{ij} = \Bigg[&\left(\frac{2G\nu}{1-2\nu}\hat{U}^S_{kj,k} + s\alpha\hat{P}^S_j\right)\delta_{i\ell} \\ &+ G\left(\hat{U}^S_{ij,\ell}+\hat{U}^S_{\ell j,i}\right)\Bigg]n_\ell\end{aligned} \tag{19a}$$

$$\hat{Q}^S_j = \kappa\hat{P}^S_{j,i}n_i \tag{19b}$$

$$\begin{aligned}\hat{T}^F_{ij} = \Bigg[&\left(\frac{2G\nu}{1-2\nu}\hat{U}^F_{k,k} + s\alpha\hat{P}^F\right)\delta_{i\ell} \\ &+ G\left(\hat{U}^F_{i,\ell}+\hat{U}^S_{\ell,i}\right)\Bigg]n_\ell\end{aligned} \tag{19c}$$

$$\hat{Q}^F = \kappa\hat{P}^F_{,i}n_i. \tag{19d}$$

The explicit expression of these 'adjoint' tractions and fluxes are

$$\begin{aligned}\hat{T}^S_{ij} = \frac{1}{2\pi}\Bigg\{&\frac{1-2\nu_u}{2(1-\nu_u)}\frac{n_i r_{,j} - n_j r_{,j} - \delta_{ij} r_{,n}}{r} \\ &-\frac{1}{1-\nu_u}\frac{r_{,i}\, r_{,j}\, r_{,n}}{r} + \frac{\nu_u-\nu}{(1-\nu)(1-\nu_u)}\lambda \\ &\times\Big[n_i r_{,j}\left(K_3(\xi)-3\xi^{-1}K_2(\xi)-2\xi^{-3}\right) \\ &+ \left(n_j r_{,i} + \delta_{ij} r_{,n}\right)\left(\xi^{-1}K_2(\xi)-2\xi^{-3}\right) \\ &+ r_{,i}\, r_{,j}\, r_{,n}\left(8\xi^{-3}-K_3(\xi)\right)\Big]\Bigg\}\end{aligned} \tag{20a}$$

$$\begin{aligned}\hat{T}^F_i = \frac{1}{2\pi}\frac{s\alpha(1-2\nu)}{2\kappa(1-\nu)}\Big[&n_i\left(K_2(\xi)+K_0(\xi)-2\xi^{-2}\right) \\ &+ r_{,i}\, r_{,n}\left(4\xi^{-2}-2K_2(\xi)\right)\Big]\end{aligned} \tag{20b}$$

$$\hat{Q}_j^S = \frac{1}{2\pi}\frac{\alpha(1-2\nu)}{2G(1-\nu)}\left[r_{,j}\,r_{,n}\,(2\xi^{-2}-K_2(\xi)) + n_j(\xi^{-1}K_1(\xi)-\xi^{-2})\right] \tag{20c}$$

$$\hat{Q}^F = -\frac{i}{2\pi}\lambda K_1(\xi)r_{,n}\,. \tag{20d}$$

Note that $r_{,n} = r_{,k}n_k$ denotes the normal derivative.

## B Convolution Quadrature Method

The 'CQM' developed by Lubich numerically approximates a convolution integral for $n = 0, 1\ \ldots, N$

$$y(t) = \int_0^t f(t-\tau)g(\tau)\mathrm{d}\tau$$

$$\rightarrow y(n\Delta t) = \sum_{k=0}^{n} w_{n-k}(\bar{\Delta} t)g(k\bar{\Delta} t), \tag{21}$$

by a quadrature rule whose weights are determined by the Laplace transformed function $\hat{f}$ and a linear multistep method. This method was originally published in [13] and [14]. Application to the boundary element method may be found in [20]. Here, a brief overview of the method is given.

In formula (21), the time $t$ is divided in $N$ equal steps $\Delta t$. The weights $w_n(\Delta t)$ are the co-efficients of the power series

$$\hat{f}\left(\frac{\gamma(z)}{\bar{\Delta} t}\right) = \sum_{n=0}^{\infty} w_n(\Delta t)z^n \tag{22}$$

with the complex variable z. The coefficients of a power series are usually calculated with Cauchy's integral formula. After a polar coordinate transformation, this integral is approximated by a trapezodial rule with $L$ equal steps $\frac{2\pi}{L}$. This leads to

$$w_n(\Delta t) = \frac{1}{2\pi i}\int_{|z|=\mathscr{R}} \hat{f}\left(\frac{\gamma(z)}{\Delta t}\right)z^{-n-1}\mathrm{d}z$$

$$\approx \frac{\mathscr{R}^{-n}}{L}\sum_{\ell=0}^{L-1}\hat{f}\left(\frac{\gamma\left(\mathscr{R}e^{i\ell\frac{2\pi}{L}}\right)}{\Delta t}\right)e^{-in\ell\frac{2\pi}{L}}, \tag{23}$$

where $\mathscr{R}$ is the radius of a circle in the domain of analyticaly of $\hat{f}(z)$.

The function $\gamma(z)$ is the quotient of the characteristic polynominals of the underlying multi-step method, e.g., for a BDF 2, $\gamma(z) = 3/2 - 2z + 1/2z^2$. The used linear multi-step method must be $A(\alpha)$-stable at infinity [14]. Experience shows that the BDF 2 is the best choice [16]. Therefore, it is used in all calculations in this paper.

If one assumes that the values of $\hat{f}(z)$ in (23) are computed with an error bounded by $\epsilon$, then the choice $L = N$ and $\mathscr{R}^N = \sqrt{\epsilon}$ yeilds an error in $w_n$ of size $\mathcal{O}(\sqrt{\epsilon})$ [13]. Several tests conducted by the first author lead to the conclusion that the parameter $\epsilon = 10^{-10}$ is the best choice for the kind of functions dealt with in this paper [19]. The assumption $L = N$ leads to a order of complexity $\mathcal{O}(N^2)$ for calculating the $N$ coefficients $w_n(\Delta t)$. Due to the exponential function at the end of formula (23) this can be reduced to $\mathcal{O}(N \log N)$ using the technique of the Fas Fourier Transformation (FFT).

## References


1. Abreu A, Carrer J, Mansur W (2003) Scalar wave propagation in 2D: a BEM formulation based on the operational quadrature method. Eng Anal Bound Ele 27:101–105
2. Antes H, Schanz M, Alvermann S (2004) Dynamic analyses of frames by integral equations for bars and timoshenko beams. J Sound Vibr 276(3–5):807–836
3. Biot M (1941) General theory of three-dimensional consolidation. J Appl Phy 12:155–164
4. Bonnet G (1987) Basic singular solutions for a poroelastic medium in the dynamic range. J Acoustical Society of America 82(5):1758–1762
5. Cheng AH-D, Detournay E (1988) A direct boundary element method for plane strain poroelasticity. Int J Numeri Anal Meth Geomech 12:551–572
6. Cheng AH-D, Detournay E (1998) On singular integral equations and fundamental solutions of poroelasticity. Int J Solids Struct 35(34–35):4521–4555
7. Dargush G, Banerjee P (1989) A time domain boundary element method for poroelasticity. Int J Numer Meth Eng 28(10):2423–2449
8. de Boer R (2000) Theory of porous media. Springer-Verlag, Berlin
9. Detournay E, Cheng AH-D (1988) Poroelastic response of a borehole in a non-hydrostatic stress field. Int J Rock Mech Mining Sci 25(3):178–182
10. Detournay E, Cheng AH-D (1993) Fundamentals of poroelasticity. Volume II of Comprehensive Rock Engineering: Principles, Practice & Projects., Chapter 5, Pergamon Press, pp 113–171
11. Domínguez J (1993) Boundary elements in dynamics. Computational Mechanics Publication, Southampton
12. Kim Y, Kingsbury H (1979) Dynamic characterization of poroelastic materials. Exp Mech 19:252–258
13. Lubich C (1988a) Convolution quadrature and discretized operational calculus. I. Numerische Mathematik 52:129–145
14. Lubich C (1988b) Convolution quadrature and discretized operational calculus. II. Numerische Mathematik 52:413–425
15. Mantič V (1993) A new formula for the C-matrix in the somigliana identity. J Elasticity 33:191–201
16. Schanz M (1999) A boundary element formulation in time domain for viscoelastic solids. Communications in Numer Meth Eng 15:799–809
17. Schanz M (2001a) Application of 3-D Boundary Element formulation to wave propagation in poroelastic solids. Eng Analy Bound Elem 25(4–5):363–376
18. Schanz M (2001b) Wave propagation in viscoelastic and poroelastic continua: A boundary element approach. Lecture Notes in Appl Mech. Springer-Verlag, Berlin, Heidelberg, New York
19. Schanz M, Antes H (1997a) Application of 'operational quadrature methods' in time domain boundary element methods. Meccanica 32(3):179–186
20. Schanz M, Antes H (1997b) A new visco- and elastodynamic time domain boundary element formulation. Comput Mech 20(5):452–459
21. Schanz M, Antes H, Rüberg T (2005) Convolution quadrature boundary element method for quasi-static visco- and poroelastic continua. Comput Struct 83:673–684

22. Schanz M, Diebels S (2003) A comparative study of Biot's theory and the linear Theory of Porous Media for wave propagation problems. Acta Mech 161(3–4):213–235
23. Zhang C (2000) Transient elastodynamic antiplane crack analysis in anisotropic solids. Int J Solids Struct 37:6107–6130
24. Zhang C (2003) Transient dynamic response of a cracked piezoelectric solid under impact loading. In :Wendland W, Efendiev M (eds.), Analysis and Simulation of Multifield Problems, Volume 12 of Lecture Notes in Appl Comput Mech. Springer-Verlag, Berlin, Heidelberg, New York, pp. 247–253
25. Zhang C, Sladek J, Sladek V (2003) Effects of material gradients on transient dynamic mode-III stress intensity factors in a FGM. Int J Solids Struct 40(20):5251–5270